

# Prospects for Strong Cavity Quantum Electrodynamics with Superconducting Circuits

S. M. Girvin<sup>1</sup>, Ren-Shou Huang<sup>1,2</sup>, Alexandre Blais<sup>1</sup>,  
Andreas Wallraff<sup>3</sup> and R. J. Schoelkopf<sup>3</sup>

<sup>1</sup>Department of Physics, Sloane Physics Laboratory, Yale University, New Haven, CT 06520-8120

<sup>2</sup>Department of Physics, Indiana University, Bloomington, IN 47405

<sup>3</sup>Department of Applied Physics, Becton Laboratory, Yale University, New Haven, CT 06520-8284

October 28, 2003

**We propose a realizable architecture using one-dimensional transmission line resonators to reach the strong coupling limit of cavity quantum electrodynamics in superconducting electrical circuits. The vacuum Rabi frequency for the coupling of cavity photons to quantized excitations of an adjacent electrical circuit (qubit) can easily exceed the damping rates of both the cavity and the qubit. This architecture is attractive for quantum computing and control, since it provides strong inhibition of spontaneous emission, potentially leading to greatly enhanced qubit lifetimes, allows high-fidelity quantum non-demolition measurements of the state of multiple qubits, and has a natural mechanism for entanglement of qubits separated by centimeter distances. In addition it would allow production of microwave photon states of fundamental importance for quantum communication.**

Cavity quantum electrodynamics (cQED) studies the properties of atoms coupled to discrete photon modes in high  $Q$  cavities. Such systems are of great interest in the study of fundamental quantum mechanics of open systems, the engineering of quantum states and the study of measurement-induced decoherence [1, 2, 3], and have also been proposed as possible candidates for use in quantum information processing and transmission [1, 2, 3]. Ideas for novel cQED analogs using nano-mechanical resonators have recently been suggested by Schwab and collaborators [4, 5]. We present a realistic proposal for cQED via Cooper pair boxes coupled to a one-dimensional (1D) transmission line resonator as shown in Fig. 1, within a simple circuit that can be fabricated on a single microelectronic chip. As we discuss, 1D cavities offer a number of practical advantages in reaching the strong coupling limit of cQED over previous proposals using discrete LC circuits [6, 7], large Josephson junctions [8, 9, 10], or 3D cavities [11, 12, 13]. Besides the potential for entangling qubits to realize two-qubit gates addressed in those works, we show that the cQED approach also gives strong and controllable isolation of the qubits from the electromagnetic environment, permits high fidelity quantum non-demolition (QND) readout of multiple qubits, and can produce states of microwave photon fields suitable for quantum communication. The proposed circuits therefore provide a simple and efficient architecture for solid-state quantum computation, in addition to opening up a new avenue for the study of entanglement and quantum measurement physics with macroscopic objects. We will frame our discussion in a way that makes contact between the language of atomic physics and that of electrical engineering, and begin with a brief general overview of cQED before turning to a more specific discussion of our proposed architecture.

In the optical version of cQED [2], one drives the cavity with a laser and monitors changes in the cavity transmission resulting from coupling to atoms falling through the cavity. One can also monitor the spontaneous emission of the atoms into transverse modes not confined by the cavity. It is not generally possible to directly determine the state of the atoms after they

have passed through the cavity because the spontaneous emission lifetime is on the scale of nanoseconds. One can, however, infer information about the state of the atoms inside the cavity from real-time monitoring of the cavity optical transmission.

In the microwave version of cQED [3] one uses a very high  $Q$  superconducting 3D resonator to couple photons to transitions in Rydberg atoms. Here one does not directly monitor the state of the photons, but is able to determine with high efficiency the state of the atoms after they have passed through the cavity (since the excited state lifetime is of order 30 ms). From this state-selective detection one can infer information about the state of the photons in the cavity.

The key parameters describing a cQED system (see Table I) are the cavity resonance frequency  $\omega_r$ , the atomic transition frequency  $\Omega$ , and the strength of the atom-photon coupling  $g$  appearing in the Jaynes-Cummings [14] Hamiltonian

$$H = \hbar\omega_r \left( a^\dagger a + \frac{1}{2} \right) + \frac{\hbar\Omega}{2} \sigma^z + \hbar g (a^\dagger \sigma^- + a \sigma^+) + H_\kappa + H_\gamma. \quad (1)$$

Here  $H_\kappa$  describes the coupling of the cavity to the continuum which produces the decay rate  $\kappa = \omega_r/Q$ , while  $H_\gamma$  describes the coupling of the atom to modes other than the cavity mode which cause the excited state to decay at rate  $\gamma$  (and possibly also produce additional dephasing effects). An additional important parameter in the atomic case is the transit time  $t_{\text{transit}}$  of the atom through the cavity. In the absence of damping and for the case of zero detuning [ $\Delta \equiv \Omega - \omega_r = 0$ ] between the atom and the cavity, an initial zero-photon excited atom state  $|0, \uparrow\rangle$  flops into a photon  $|1, \downarrow\rangle$  and back again at the vacuum Rabi frequency  $g/\pi$ . The degeneracy of the two corresponding states with  $n$  additional photons is split by  $2\hbar g\sqrt{n+1}$ . Equivalently, the atom's state and the photon number are entangled. The value of  $g = \mathcal{E}_{\text{rms}}d/\hbar$  is determined by the transition dipole moment  $d$  and the rms zero-point electric field of the cavity mode. Strong coupling is achieved when  $g \gg \kappa, \gamma$  [15].

We now consider in more specific detail the cQED setup illustrated in Fig. 1. A number

of possible superconducting quantum circuits could function as the ‘atom’. For definiteness we focus on the Cooper pair box [16, 6, 17, 18]. Unlike the usual cQED case, these artificial ‘atoms’ remain at fixed positions indefinitely and so do not suffer from the problem that the coupling  $g$  varies with position in the cavity. An additional advantage is that the zero-point energy is distributed over a very small effective volume ( $\approx 10^{-5}$  cubic wavelengths) for our choice of a quasi-one-dimensional transmission line ‘cavity.’ This leads to significant rms voltages  $V_{\text{rms}}^0 \sim \sqrt{\hbar\omega_r/cL}$  between the center conductor and the adjacent ground plane at the antinodal positions, where  $L$  is the resonator length and  $c$  is the capacitance per unit length of the transmission line. At a resonant frequency of 10 GHz ( $\hbar\nu/k_B \sim 0.5$  K) and for a  $10\ \mu\text{m}$  gap between the center conductor and the adjacent ground plane,  $V_{\text{rms}} \sim 2\ \mu\text{V}$  corresponding to electric fields  $\mathcal{E}_{\text{rms}} \sim 0.2\ \text{V/m}$ , some 100 times larger than achieved in the 3D cavity described in Ref. [3]. Thus, this geometry might also be useful for coupling to Rydberg atoms [19].

In addition to the small effective volume, and the fact that the on-chip realization of cQED shown in Fig. 1 can be fabricated with existing lithographic techniques, a transmission-line resonator geometry offers other practical advantages over LC circuits or large Josephson junctions. The qubit can be placed within the cavity formed by the transmission line to strongly suppress the spontaneous emission, in contrast to an LC circuit, where radiation and parasitic resonances may be induced in the wiring. Since the resonant frequency of the transmission line is determined primarily by a fixed geometry, its reproducibility and immunity to  $1/f$  noise should be superior to Josephson junction resonators. Finally, transmission line resonances in coplanar waveguides with  $Q \sim 10^6$  have already been demonstrated [20], suggesting that the internal losses can be very low. The optimal choice of the resonator  $Q$  in this approach is strongly dependent on the presently unknown intrinsic decay rates of superconducting qubits. Here we assume the conservative case of an overcoupled resonator with a  $Q \sim 10^4$ , which is preferable for the first experiments.

Our choice of ‘atom’, the Cooper pair box [16, 6] is a mesoscopic superconducting grain with a significant charging energy. The two lowest charge states having  $N_0$  and  $N_0 + 1$  Cooper pairs are coherently mixed by Josephson tunnelling between the box and a reservoir (in this case the resonator ground plane) leading to the two-level Hamiltonian [6]

$$H_Q = E_{\text{el}}\sigma^x - \frac{E_J}{2}\sigma^z. \quad (2)$$

Here, we have chosen the spinor basis such that the box Cooper pair number operator is [21]  $\hat{N} - N_0 = (1 + \sigma^x)/2$ . The electrostatic energy is given by  $4E_c(C_g V_g/2e - 1/2)$ , where  $C_g$  is the coupling capacitance between the box and the resonator,  $E_c \equiv e^2/2C_\Sigma$  is the charging energy determined by the total box capacitance and  $E_J$  is the Josephson energy. Dc gating of the box can be conveniently achieved by applying a bias voltage to the center conductor of the transmission line. In addition to the dc part  $V_g^{\text{dc}}$  the gate voltage has a quantum part  $v = V_{\text{rms}}^0(a^\dagger + a)$  from which we obtain

$$g = \frac{E_J}{\sqrt{E_J^2 + E_{\text{el}}^2}} \frac{e}{\hbar} \beta \sqrt{\frac{\hbar\omega_r}{cL}}, \quad (3)$$

where  $\beta \equiv C_g/C_\Sigma$ . At the charge degeneracy point  $E_{\text{el}} = 0$  (where  $n_g = C_g V_g^{\text{dc}}/2e = 1/2$ ), the two levels are split only by the Josephson energy and the ‘atom’ is highly polarizable, having transition dipole moment  $d \equiv \hbar g/\mathcal{E}_{\text{rms}} \sim 2 \times 10^4$  atomic units ( $ea_0$ ), or more than an order of magnitude larger than even a typical Rydberg atom [15]. An experimentally realistic [18] coupling  $\beta \sim 0.1$  leads to a vacuum Rabi rate  $g/\pi \sim 100$  MHz, which is three orders of magnitude larger than in corresponding atomic microwave cQED experiments [3].

A comparison of the experimental parameters for implementations of cavity QED with optical and microwave atomic systems, and for the proposed implementation with superconducting circuits, is presented in Table I. We assume a relatively low  $Q = 10^4$  and a worst case estimate, consistent with the bound set by previous experiments (discussed further below), for the intrinsic qubit lifetime of  $1/\gamma \geq 2 \mu\text{s}$ . The standard figures of merit [22] for strong coupling are the

critical photon number needed to saturate the atom on resonance  $m_0 = \gamma^2/2g^2 \leq 1 \times 10^{-6}$  and the minimum atom number detectable by measurement of the cavity output  $N_0 = 2\gamma\kappa/g^2 \leq 6 \times 10^{-5}$ . These remarkably low values are clearly very favorable, and show that superconducting circuits could access the interesting regime of very strong coupling.

For the case of zero detuning and weak coupling  $g < \kappa$ , the radiative decay rate of the qubit into the transmission line becomes strongly *enhanced* by a factor of  $Q$  relative to the rate in the absence of the cavity [15] because of the resonant enhancement of the density of states at the atomic transition frequency. In electrical engineering language, the  $\sim 50 \Omega$  external transmission line impedance is transformed on resonance to a high value which is better matched to extract energy from the qubit. For strong coupling, the first excited state becomes a doublet with line width  $(\kappa + \gamma)/2$  since the excitation is half atom and half photon [15]. As can be seen from Table I, the coupling is so strong that, even for the low  $Q = 10^4$  we have assumed,  $2g/(\kappa + \gamma) \sim 100$  vacuum Rabi oscillations are possible, and the frequency splitting ( $g/\pi \sim 100$  MHz) will be readily resolvable in the transmission spectrum of the resonator. This spectrum can be observed in the same manner employed in optical atomic experiments, with a continuous wave measurement at low drive, and will be of practical use to find the dc gate voltage needed to tune the box into resonance with the cavity. Of more fundamental importance than this simple avoided level crossing however, is the fact that the Rabi splitting scales with the square root of the photon number, making the level spacing anharmonic. This should cause a number of novel non-linear effects [14] to appear in the spectrum at higher drive powers when the average photon number in the cavity is large ( $\langle n \rangle > 1$ ). A conservative estimate of the noise energy for a 10 GHz cryogenic high electron mobility (HEMT) amplifier is  $n_{\text{amp}} = k_B T_N / \hbar \omega = 100$  photons, so these spectral features should be readily observable in a measurement time  $t_{\text{meas}} = n_{\text{amp}} / \langle n \rangle \kappa$ , or only  $\sim 16 \mu\text{s}$  for  $\langle n \rangle \sim 1$ .

For the case of strong detuning, the coupling to the continuum is substantially reduced. One

can view the effect of the detuned resonator as filtering out the vacuum noise at the qubit transition frequency or, in electrical engineering terms, as providing an impedance transformation which strongly *reduces* the real part of the environmental impedance seen by the qubit. For large detuning the qubit excitation spends only a small fraction of its time as a photon [15] so that the decay rate into the transmission line is only  $\gamma_\kappa = (g/\Delta)^2 \kappa \sim 1/(64 \mu\text{s})$ , much less than  $\kappa$ .

One of the important motivations for this cQED experiment is to determine the various contributions to the qubit decay rate  $\gamma$  so that we can understand their fundamental physical origins as well as engineer improvements. Besides  $\gamma_\kappa$ , there are two additional contributions to  $\gamma = \gamma_\kappa + \gamma_\perp + \gamma_{\text{NR}}$ . Here  $\gamma_\perp$  is the decay rate into photon modes other than the cavity mode, and  $\gamma_{\text{NR}}$  is the rate of other (possibly non-radiative) decays. Optical cavities are relatively open and  $\gamma_\perp$  is significant, but for 1D microwave cavities,  $\gamma_\perp$  is expected to be negligible (despite the very large transition dipole). For Rydberg atoms the two qubit states are both highly excited levels and  $\gamma_{\text{NR}}$  represents (radiative) decay out of the two-level subspace. For Cooper pair boxes,  $\gamma_{\text{NR}}$  is completely unknown at the present time, but could have contributions from phonons, two-level systems in insulating [23] barriers and substrates, or thermally excited quasiparticles.

For Cooper box qubits *not* inside a cavity, recent experiments [18] have determined a relaxation time  $1/\gamma = T_1 \sim 1.3 \mu\text{s}$  despite the back action of continuous measurement by a SET electrometer. Vion et al. [17] found  $T_1 \sim 1.84 \mu\text{s}$  (without measurement back action) for their charge-phase qubit. The rate of relaxation expected from purely vacuum noise (spontaneous emission) is [18, 6]

$$\gamma_\kappa = \frac{E_J^2}{E_J^2 + E_{\text{el}}^2} \left(\frac{e}{\hbar}\right)^2 \beta^2 2\hbar\Omega \text{Re}[Z(\Omega)]. \quad (4)$$

It is difficult in most experiments to precisely determine the real part of the high frequency environmental impedance  $Z(\Omega)$  presented by the leads connected to the qubit, but reasonable estimates [18] yield values of  $T_1$  in the range of  $1 \mu\text{s}$ . Thus in these experiments, if there are

non-radiative decay channels, they are at most comparable to the vacuum radiative decay rate (and may well be much less). Experiments with a cavity will present the qubit with a simple and well controlled electromagnetic environment, in which the radiative lifetime can be enhanced with detuning to  $1/\gamma_\kappa > 64 \mu\text{s}$ , allowing  $\gamma_{\text{NR}}$  to dominate and yielding valuable information about any non-radiative processes.

For large detuning, making the unitary transformation  $U = \exp\left[(g/\Delta)(a\sigma^+ - a^\dagger\sigma^-)\right]$  and expanding to second order in  $g$ , approximately diagonalizes the Hamiltonian (neglecting damping for the moment)

$$UHU^\dagger \approx \hbar \left[ \omega_r + \frac{g^2}{\Delta} \sigma^z \right] a^\dagger a + \frac{1}{2} \hbar \left[ \Omega + \frac{g^2}{\Delta} \right] \sigma^z. \quad (5)$$

We see that there is a dispersive shift of the cavity transition by  $\sigma_z g^2/\Delta$ , that is the qubit pulls the cavity frequency by  $\pm g^2/\kappa\Delta = \pm 2.5$  line widths for a 10% detuning. Exact diagonalization [15] shows that the pull becomes power dependent and decreases in magnitude for cavity photon numbers on the scale  $n = n_{\text{crit}} \equiv \Delta^2/4g^2 \sim 100$ . In the regime of non-linear response, single-atom optical bistability [14] can be expected when the drive frequency is off resonance at low power but on resonance at high power [24].

The state-dependent pull of the cavity frequency by the qubit can be used to entangle the state of the qubit with that of the photons passing through the resonator. For  $g^2/\kappa\Delta > 1$  the pull is greater than the line width and the microwave frequency can be chosen so that the transmission of the cavity is close to unity for one state of the qubit and close to zero for the other [25]. For  $g^2/\kappa\Delta \ll 1$  the state of the qubit is encoded in the phase of the transmitted microwaves. An initial qubit state  $|\chi\rangle = \alpha|\uparrow\rangle + \beta|\downarrow\rangle$  evolves under microwave illumination into the entangled state  $|\psi\rangle = \alpha|\uparrow, \theta\rangle + \beta|\downarrow, -\theta\rangle$ , where  $\tan \theta = 2g^2/\kappa\Delta$ , and  $|\pm\theta\rangle$  are (interaction representation) coherent states with the appropriate mean photon number and opposite phases. Such an entangled state can be used to couple qubits in distant resonators and allow quantum

communication [26]. If an independent measurement of the qubit state can be made, then such states can be turned into photon Schrödinger cats [15].

The phase shift of the transmitted microwaves can be measured using standard heterodyne techniques, and can therefore serve as a high efficiency quantum non-demolition dispersive readout of the state of the qubit, as described in Figure 2. Exciting the cavity to a maximal amplitude  $n_{\text{crit}} = 100 \sim n_{\text{amp}}$  the signal-to-noise ratio,  $\text{SNR} = (n_{\text{crit}}/n_{\text{amp}})(\kappa/\gamma)$ , can be very high if the qubit lifetime is longer than a few cavity decay times ( $1/\kappa = 160$  ns). We see from Eq. (5) that the ac-Stark/Lamb shift of the box transition is  $(2g^2/\Delta)(n + 1/2)$ , so the back action of the dispersive cQED measurement is due to quantum fluctuations of the number of photons in the cavity which cause variations in the ac Stark shift, that dephase the qubit. A second possible form of back action is mixing transitions between the two qubit states induced by the microwaves. Since the coupling is so strong, large detuning  $\Delta = 0.1 \omega_r$  can be chosen, making the mixing rate limited not by the frequency spread of the drive pulse, but rather by the width of the qubit excited state itself. The rate of driving the qubit from ground to excited state when  $n$  photons are in the cavity is  $R \approx n(g/\Delta)^2\gamma$ . If the measurement pulse excites the cavity to  $n = n_{\text{crit}}$ , we see that the excitation rate is still only 1/4 of the relaxation rate, so the main limitation on the fidelity of the QND readout is the decay of the excited state of the qubit during the course of the readout. This occurs (for small  $\gamma$ ) with probability  $P_{\text{relax}} \sim \gamma t_{\text{meas}} \sim 5 \times \gamma/\kappa \sim 1.5\%$  and the measurement is highly non-demolition. The numerical stochastic wave function calculations [27] shown in Fig. 2 confirm that the measurement-induced mixing is negligible and that one can determine the qubit's state in a single-shot measurement with high fidelity. The readout fidelity, including the effects of this stochastic decay, and related figures of merit of the QND readout are summarized in Table II. Since nearly all the energy used in this dispersive measurement scheme is dissipated in the remote terminations of the input and output transmission lines, it has the practical advantage of avoiding quasiparticle generation in

the qubit.

Another key feature of the cavity QED readout is that it lends itself naturally to operation of the box at the charge degeneracy point ( $n_g = 1/2$ ), where it has been shown that  $T_2$  can be enormously enhanced [17] because the energy splitting has an extremum with respect to gate voltage and isolation of the qubit from  $1/f$  dephasing is optimal. The derivative of the energy splitting with respect to gate voltage is the charge difference in the two qubit states. At the degeneracy point this derivative vanishes and the environment cannot distinguish the two states and thus cannot dephase the qubit. This also implies that a charge measurement cannot be used to determine the state of the system [4, 5]. While the first derivative of the energy splitting with respect to gate voltage vanishes at the degeneracy point, the second derivative, corresponding to the difference in charge *polarizability* of the two quantum states, is *maximal*. One can think of the qubit as a non-linear quantum system having a state-dependent capacitance (or in general, an admittance) which changes sign between the ground and excited states [28]. It is this change in polarizability which is measured in the dispersive QND measurement.

In contrast, standard charge measurement schemes [29, 18] require moving away from the optimal point. Simmonds et al. [23] have recently raised the possibility that there are numerous parasitic environmental resonances which can relax the qubit when its frequency  $\Omega$  is changed during the course of moving the operating point. The dispersive cQED measurement is therefore highly advantageous since it operates best at the charge degeneracy point. In general, such a measurement of an ac property of the qubit is strongly desirable in the usual case where dephasing is dominated by low frequency ( $1/f$ ) noise. Notice also that the proposed quantum non-demolition measurement would be the inverse of the atomic microwave cQED measurement in which the state of the photon field is inferred non-destructively from the phase shift in the state of atoms sent through the cavity [3].

Finally, the transmission-line resonator has the advantage that it should be possible to place

multiple qubits along its length ( $\sim 1$  cm) and entangle them together, which is an essential requirement for quantum computation. For the case of two qubits, they can be placed closer to the ends of the resonator but still well isolated from the environment and can be separately dc biased by capacitive coupling to the left and right center conductors of the transmission line. Any additional qubits would have to have separate gate bias lines installed. If qubits  $i$  and  $j$  are tuned in resonance with each other but detuned from the cavity, the effective Hamiltonian will contain qubit-qubit coupling due to exchange of virtual photons:  $H_2 = (g^2/\Delta)(\sigma_i^+ \sigma_j^- + \sigma_i^- \sigma_j^+)$ . Starting with an excitation in one of the qubits, this interaction will have the pair of qubits maximally entangled after a time  $t_{\sqrt{i\text{SWAP}}} = \pi\Delta/4g^2 \sim 50$  ns. Making the most optimistic assumption that we can take full advantage of the lifetime enhancement inside the cavity (i.e. that  $\gamma_{\text{NR}}$  can be made negligible), the number of  $\sqrt{i\text{SWAP}}$  operations which can be carried out in one cavity decay time is  $N_{\text{op}} = 4\Delta/\pi\kappa \sim 1200$  for the experimental parameters assumed above. This can be further improved if the qubit's non-radiative decay is sufficiently small, and higher  $Q$  cavities are employed. When the qubits are detuned from each other, the qubit-qubit interaction in the effective Hamiltonian is turned off, hence the coupling is tunable. Numerical simulations indicate that when the qubits are strongly detuned from the cavity, single-bit gate operations can be performed with high fidelity [24]. Driving the cavity at its resonance frequency constitutes a *measurement* because the phase shift of the transmitted wave is strongly dependent on the state of the qubit and hence the photons become entangled with the qubit. On the other hand, driving the cavity at the qubit transition frequency constitutes a *rotation*. This is *not* a measurement because, for large detuning the photons are largely reflected with a phase shift which is independent of the state of the qubit. Hence there is little entanglement and the rotation fidelity is high [24].

Together with one-qubit gates, the interaction  $H_2$  is sufficient for universal quantum computation (UQC) [30]. Alternatively,  $H_2$  can be used to realize encoded UQC on the subspace

$\mathcal{L} = \{|\uparrow\downarrow\rangle, |\downarrow\uparrow\rangle\}$  [31]. In this context, a simpler non-trivial encoded two-qubit gate can also be obtained by tuning, for a time  $t = \pi\Delta/3g^2$ , all four qubits in the pair of encoded logical qubits in resonance with each other but detuned from the resonator. This is closely related to the Sørensen-Mølmer scheme discussed in the context of the ion-trap proposals [32]. Interestingly,  $\mathcal{L}$  is also a decoherence-free subspace with respect to global dephasing [31] and use of this encoding will provide some protection against noise.

Another advantage of the dispersive QND readout is that one may be able to determine the state of multiple qubits in a single shot without the need for additional signal ports. For example, for the case of two qubits with different detunings, the cavity pull will take on four different values  $\pm g_1^2/\Delta_1 \pm g_2^2/\Delta_2$  allowing single-shot readout of the coupled system. This can in principle be extended to  $N$  qubits provided that the range of individual cavity pulls can be made large enough to distinguish all the combinations. Alternatively, one could read them out in small groups at the expense of having to electrically vary the detuning of each group to bring them into strong coupling with the resonator.

In summary, we propose that the combination of one-dimensional superconducting transmission line resonators, which confine their zero point energy to extremely small volumes, and superconducting charge qubits, which are electrically controllable qubits with large electric dipole moments, constitutes an interesting system to access the strong-coupling regime of cavity quantum electrodynamics. This combined system constitutes an advantageous architecture for the coherent control, entanglement, and readout of quantum bits for quantum computation and communication. Among the practical benefits of this approach are the ability to suppress radiative decay of the qubit while still allowing one-bit operations, a simple and minimally disruptive method for readout of single and multiple qubits, and the ability to generate tunable two-qubit entanglement over centimeter-scale distances. We also note that in the structures described here, the emission or absorption of a single photon by the qubit is tagged by a sudden

large change in the resonator transmission properties [24] making them potentially useful as single photon sources and detectors.

## References and Notes

- [1] H. Mabuchi, A. Doherty, *Science* **298**, 1372 (2002).
- [2] C. J. Hood, T. W. Lynn, A. C. Doherty, A. S. Parkins, H. J. Kimble, *Science* **287**, 1447 (2000).
- [3] J. Raimond, M. Brune, S. Haroche, *Rev. Mod. Phys.* **73**, 565 (2001).
- [4] A. Armour, M. Blencowe, K. C. Schwab, *Phys. Rev. Lett.* **88**, 148301 (2002).
- [5] E. K. Irish, K. Schwab, Quantum measurement of a coupled nanomechanical resonator – Cooper-pair box system (2003). cond-mat/0301252.
- [6] Y. Makhlin, G. Schön, A. Shnirman, *Rev. Mod. Phys.* **73**, 357 (2001).
- [7] O. Buisson, F. Hekking, *Macroscopic Quantum Coherence and Quantum Computing*, D. V. Averin, B. Ruggiero, P. Silvestrini, eds. (Kluwer, New York, 2001).
- [8] F. Marquardt, C. Bruder, *Phys. Rev. B* **63**, 054514 (2001).
- [9] F. Plastina, G. Falci, *Phys. Rev. B* **67**, 224514 (2003).
- [10] A. Blais, A. Maassen van den Brink, A. Zagoskin, *Phys. Rev. Lett.* **90**, 127901 (2003).
- [11] W. Al-Saidi, D. Stroud, *Phys. Rev. B* **65**, 014512 (2001).
- [12] C.-P. Yang, S.-I. Chu, S. Han, *Phys. Rev. A* **67**, 042311 (2003).
- [13] J. Q. You, F. Nori, *Phys. Rev. B* **68**, 064509 (2003).

- [14] D. Walls, G. Milburn, *Quantum optics* (Springer-Verlag, Berlin, 1994).
- [15] S. Haroche, *Fundamental Systems in Quantum Optics*, J. Dalibard, J. Raimond, J. Zinn-Justin, eds. (Elsevier, 1992), p. 767.
- [16] V. Bouchiat, D. Vion, P. Joyez, D. Esteve, M. Devoret, *Physica Scripta* **T76**, 165 (1998).
- [17] D. Vion, *et al.*, *Science* **296**, 886 (2002).
- [18] K. Lehnert, *et al.*, *Phys. Rev. Lett.* **90**, 027002 (2003).
- [19] A. S. Sorensen, C. H. van der Wal, L. Childress, M. D. Lukin, Capacitive coupling of atomic systems to mesoscopic conductors (2003). (quant-ph/0308145).
- [20] P. K. Day, H. G. LeDuc, B. A. Mazin, A. Vayonakis, J. Zmuidzinas, *Nature (London)* **425**, 817 (2003).
- [21] For a large ratio of  $E_J/E_c$  higher charge states will be mixed into the two lowest energy eigenstates and the coefficient of  $\sigma_x$  in this expression will be somewhat different from unity.
- [22] H. Kimble, *Structure and dynamics in cavity quantum electrodynamics* (Academic Press, 1994).
- [23] R. W. Simmonds, K. M. Lang, D. A. Hite, D. P. Pappas, J. Martinis, Decoherence in Josephson qubits from junction resonances (2003). Submitted to Phys. Rev. Lett.
- [24] S. Girvin, A. Blais, R. Huang. Unpublished.
- [25] We note that for the case of  $Q = 10^6$ , the cavity pull is a remarkable  $\pm 250$  line widths, but, depending on the non-radiative decay rate of the qubit, this may be in the regime  $\kappa < \gamma$ , making the state measurement too slow.

- [26] S. van Enk, J. Cirac, P. Zoller, *Science* **279**, 2059 (1998).
- [27] R. Schack, T. A. Brun, *Comp. Phys. Comm.* **102**, 210 (1997).
- [28] D. Averin, C. Bruder, *Phys. Rev. Lett.* **91**, 057003 (2003).
- [29] Y. Nakamura, Y. Pashkin, J. Tsai, *Nature (London)* **398**, 786 (1999).
- [30] A. Barenco, *et al.*, *Phys. Rev. A* **52**, 3457 (1995).
- [31] D. Lidar, L.-A. Wu, *Phys. Rev. Lett.* **88**, 017905 (2002).
- [32] A. Sørensen, K. Mølmer, *Phys. Rev. Lett.* **82**, 1971 (1999).

33. We are grateful to David DeMille and Michel Devoret for numerous conversations. This work was supported in part by the National Security Agency (NSA) and Advanced Research and Development Activity (ARDA) under Army Research Office (ARO) contract number DAAD19-02-1-0045, NSF DMR-0196503, the David and Lucile Packard Foundation, the W.M. Keck Foundation, NSERC and the Canadian Foundation for Innovation.

parameter	symbol	3D optical	3D microwave	1D circuit
resonance/transition frequency	$\omega_r/2\pi, \Omega/2\pi$	350 THz	51 GHz	10 GHz
vacuum Rabi frequency	$g/\pi, g/\omega_r$	220 MHz, $3 \times 10^{-7}$	47 kHz, $1 \times 10^{-7}$	100 MHz, $5 \times 10^{-3}$
transition dipole	$d/ea_0$	$\sim 1$	$1 \times 10^3$	$2 \times 10^4$
cavity lifetime	$1/\kappa, Q$	10 ns, $3 \times 10^7$	1 ms, $3 \times 10^8$	160 ns, $10^4$
atom lifetime	$1/\gamma$	61 ns	30 ms	$2 \mu\text{s}$
atom transit time	$t_{\text{transit}}$	$\geq 50 \mu\text{s}$	$100 \mu\text{s}$	$\infty$
critical atom number	$N_0 = 2\gamma\kappa/g^2$	$6 \times 10^{-3}$	$3 \times 10^{-6}$	$\leq 6 \times 10^{-5}$
critical photon number	$m_0 = \gamma^2/2g^2$	$3 \times 10^{-4}$	$3 \times 10^{-8}$	$\leq 1 \times 10^{-6}$
# of vacuum Rabi flops	$n_{\text{Rabi}} = 2g/(\kappa + \gamma)$	$\sim 10$	$\sim 5$	$\sim 10^2$

Table 1: Comparison of key rates and cQED parameters for optical [2] and microwave [3] atomic systems using 3D cavities, compared against the proposed approach using superconducting circuits, showing the possibility for attaining the strong cavity QED limit ( $n_{\text{Rabi}} \gg 1$ ). For the 1D superconducting system, a full-wave ( $L = \lambda$ ) resonator,  $\omega_r/2\pi = 10$  GHz, a relatively low  $Q$  of  $10^4$  and coupling  $\beta = C_g/C_\Sigma = 0.1$  are assumed. For the 3D microwave case, the number of Rabi flops is limited by the transit time. For the 1D circuit case, the intrinsic Cooper-pair box decay rate is unknown; a conservative value equal to the current experimental upper bound  $1/\gamma \geq 2 \mu\text{s}$  is assumed.

parameter	symbol	1D circuit
dimensionless cavity pull	$g^2/\kappa\Delta$	2.5
cavity-enhanced lifetime	$\gamma_\kappa^{-1} = (\Delta/g)^2\kappa^{-1}$	$64 \mu\text{s}$
readout SNR	$\text{SNR} = (n_{\text{crit}}/n_{\text{amp}})\kappa/\gamma$	400 (12.5)
readout error	$P_{\text{relax}} \sim 5 \times \gamma/\kappa$	1.5 % (14 %)
1 bit operation time	$T_\pi > 1/\Delta$	$> 0.16$ ns
entanglement time	$t_{\sqrt{i\text{SWAP}}} = \pi\Delta/4g^2$	$\sim 0.05 \mu\text{s}$
2 bit operations	$N_{\text{op}} = 1/[\gamma t_{\sqrt{i\text{SWAP}}}]$	$> 1200$ (40)

Table 2: Figures of merit for readout and multi-qubit entanglement of superconducting qubits using dispersive (off-resonant) coupling to a 1D transmission line resonator. The same parameters as Table 1, and a detuning of the Cooper pair box from the resonator of 10% ( $\Delta = 0.1 \omega_r$ ), are assumed. Quantities involving the qubit decay  $\gamma$  are computed both for the theoretical lower bound  $\gamma = \gamma_\kappa$  for spontaneous emission via the cavity, and (in parentheses) for the current experimental upper bound  $1/\gamma \geq 2 \mu\text{s}$ . Though the signal-to-noise of the readout is very high in either case, the estimate of the readout error rate is dominated by the probability of qubit relaxation during the measurement, which has a duration of a few cavity lifetimes ( $\sim 1 - 10 \kappa^{-1}$ ). If the qubit non-radiative decay is low, both high efficiency readout and more than  $10^3$  two-bit operations could be attained.

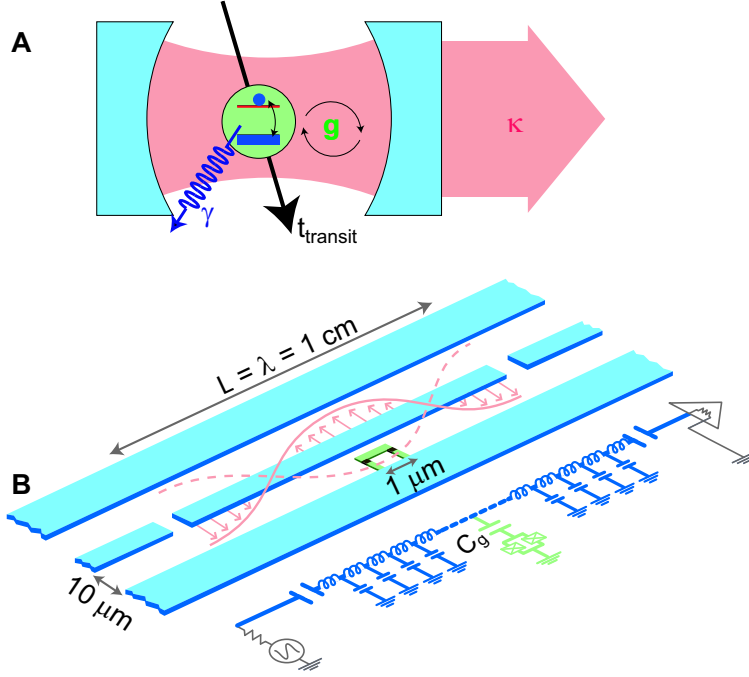


Figure 1: a) Standard representation of cavity quantum electrodynamics system, comprising a single mode of the electromagnetic field in a cavity with decay rate  $\kappa$  coupled with a coupling strength  $g = \mathcal{E}_{\text{rms}}d/\hbar$  to a two-level system with spontaneous decay rate  $\gamma$  and cavity transit time  $t_{\text{transit}}$ . b) Schematic layout and effective circuit of proposed implementation of cavity QED using superconducting circuits. The 1D transmission line resonator consists of a full-wave section of superconducting coplanar waveguide, which may be lithographically fabricated using conventional optical lithography. A Cooper-pair box qubit is placed between the superconducting lines, and is capacitively coupled to the center trace at a maximum of the voltage standing wave, yielding a strong electric dipole interaction between the qubit and a single photon in the cavity. The box consists of two small ( $\sim 100 \text{ nm} \times 100 \text{ nm}$ ) Josephson junctions, configured in a  $\sim 1 \mu\text{m}$  loop to permit tuning of the effective Josephson energy by magnetic field. Input and output signals are coupled to the resonator, via the capacitive gaps in the center line, from  $50 \Omega$  transmission lines which allow measurements of the amplitude and phase of the cavity transmission, and the introduction of dc and rf pulses to manipulate the qubit states. Multiple qubits (not shown) can be similarly placed at different antinodes of the standing wave to generate entanglement and two-bit quantum gates across distances of several millimeters.

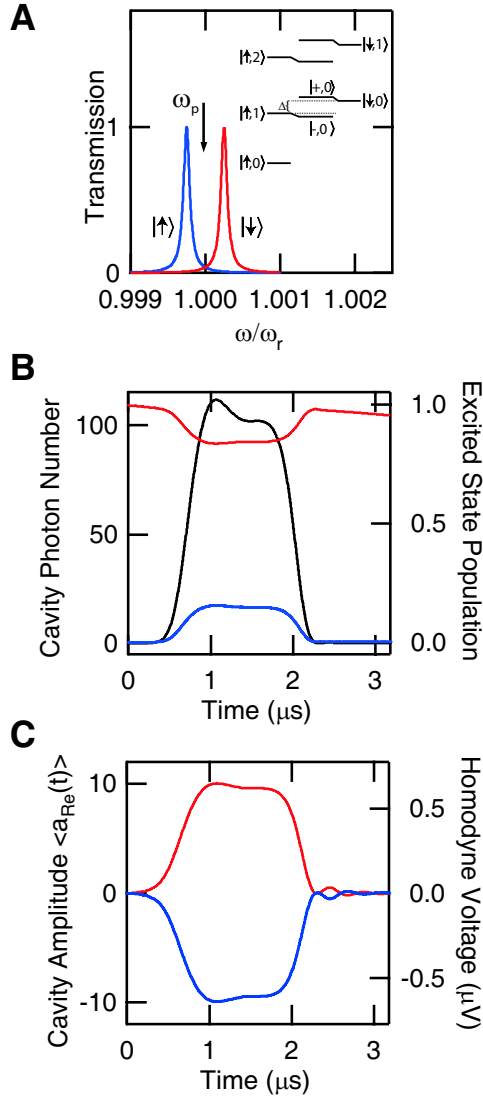


Figure 2: Use of the coupling between a Cooper-pair box qubit and a transmission-line resonator to perform a dispersive quantum non-demolition measurement. a) Transmission spectrum of the cavity, which is "pulled" by an amount  $\pm g^2/\Delta = 2.5 \times 10^{-4} \times \omega_r$ , depending on the state of the qubit (red for the excited state, blue for the ground state). To perform a measurement of the qubit, a pulse of microwave photons, at a probe frequency  $\omega_p = \omega_r$ , is sent through the cavity. Inset shows the dressed-state picture of energy levels for the cavity-qubit system, for 10% detuning. b) Results of numerical simulations of this QND readout using the quantum state diffusion method. A microwave pulse with duration  $\sim 1.5 \mu\text{s}$  excites the cavity to an amplitude  $\langle n \rangle \sim 100$ . The intracavity photon number (left axis, in black), and occupation probability of the excited state, for the case in which the qubit is initially in the ground (blue) or excited (red) state, are shown as a function of time. Though the qubit states are coherently mixed during the pulse, the probability of real transitions is seen to be small. Depending on the qubit's state, the pulse is either above or below the combined cavity-qubit resonance, and so is transmitted with a large relative phase shift that can be detected with homodyne detection. c) The real component of the cavity electric field amplitude (left axis), and the transmitted voltage phasor (right axis) in the output transmission line, for the two possible qubit states. The opposing phase shifts cause a change in sign of the output, which can be measured with high signal-to-noise to realize a single-shot, QND measurement of the qubit.